The Structure of the Pulsar Magnetosphere

S. Shibata (Yamagata University)

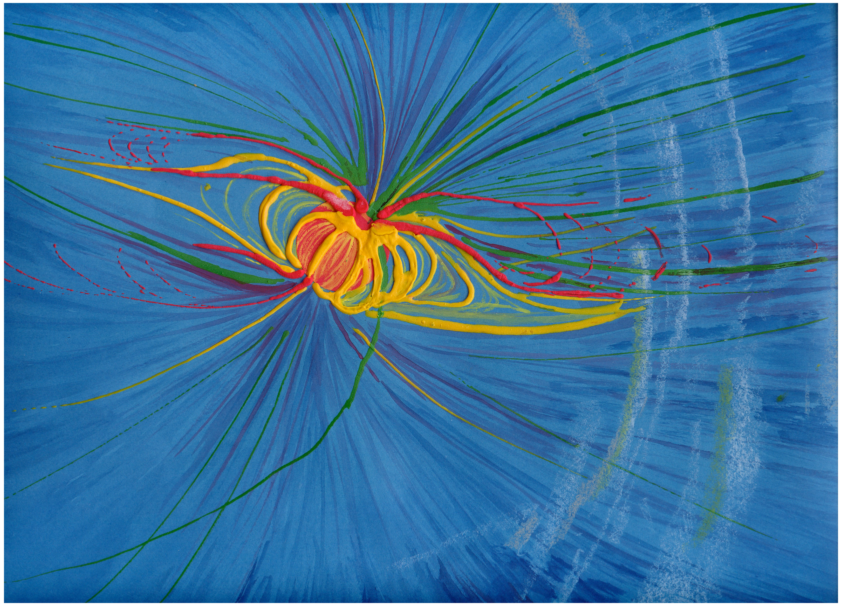

「日本SKAパルサー・突発天体研究会」, 2018年1月5日 〜 7日, 茨城県鹿嶋市　ホテルがんけ

related object

source of energy

	magnetic field	Kinetic energy of rotation	gravity
BH		Kerr BH	Accretion Powered BH
NS	Magnetar	Rotation Powered Pulsar	MSP,BW,NS+NS Accretion Powered Pulsar
WD		WD pulsar	(+nuclear fusion) CV (cataclysmic variables) SN Ia
source of matter		surface of ★ pair creation	accretion

Rotation Powered Pulsars

Observations

Gamma-ray pulsed emission
GeV bands

Fermi
Gamma-ray
Space Telescope

launched on on June 11, 2008 at 12:05 pm EDT.

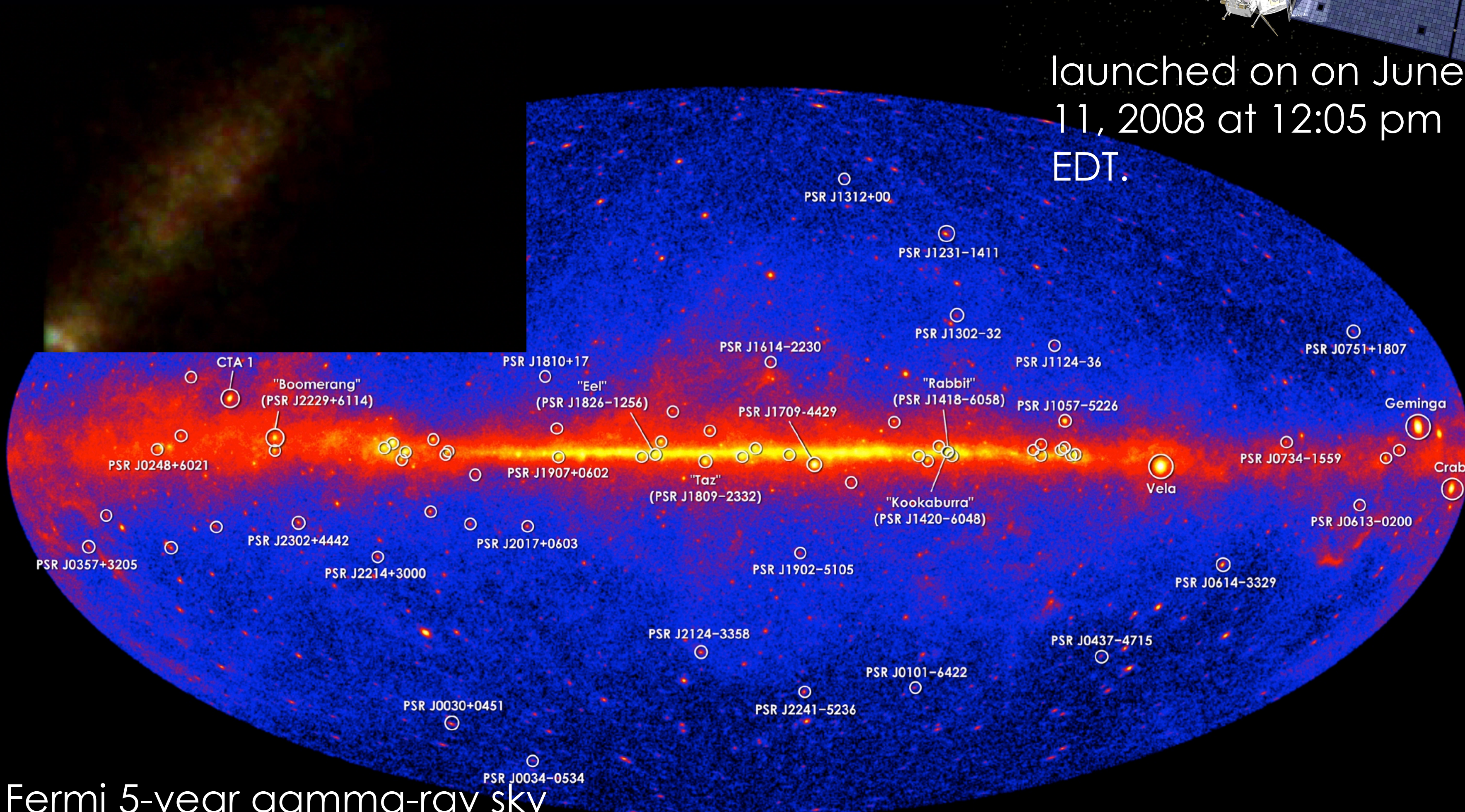

Fermi 5-year gamma-ray sky

Intensive radio pulses (more than 2600 PSRs)

T_b can be 10^{30}K

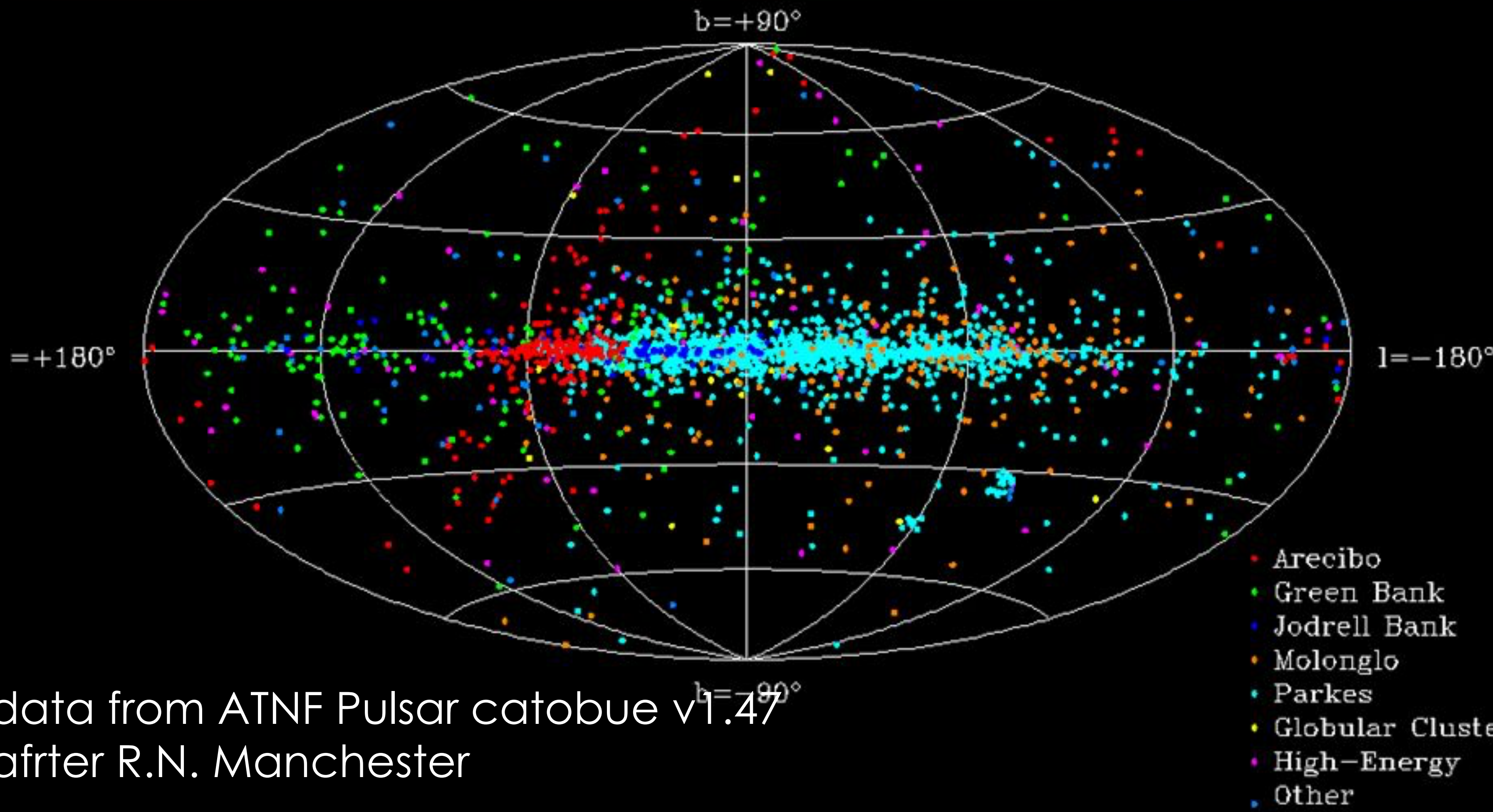

data from ATNF Pulsar catobue v1.47
afrter R.N. Manchester

X-ray Images of PWNe

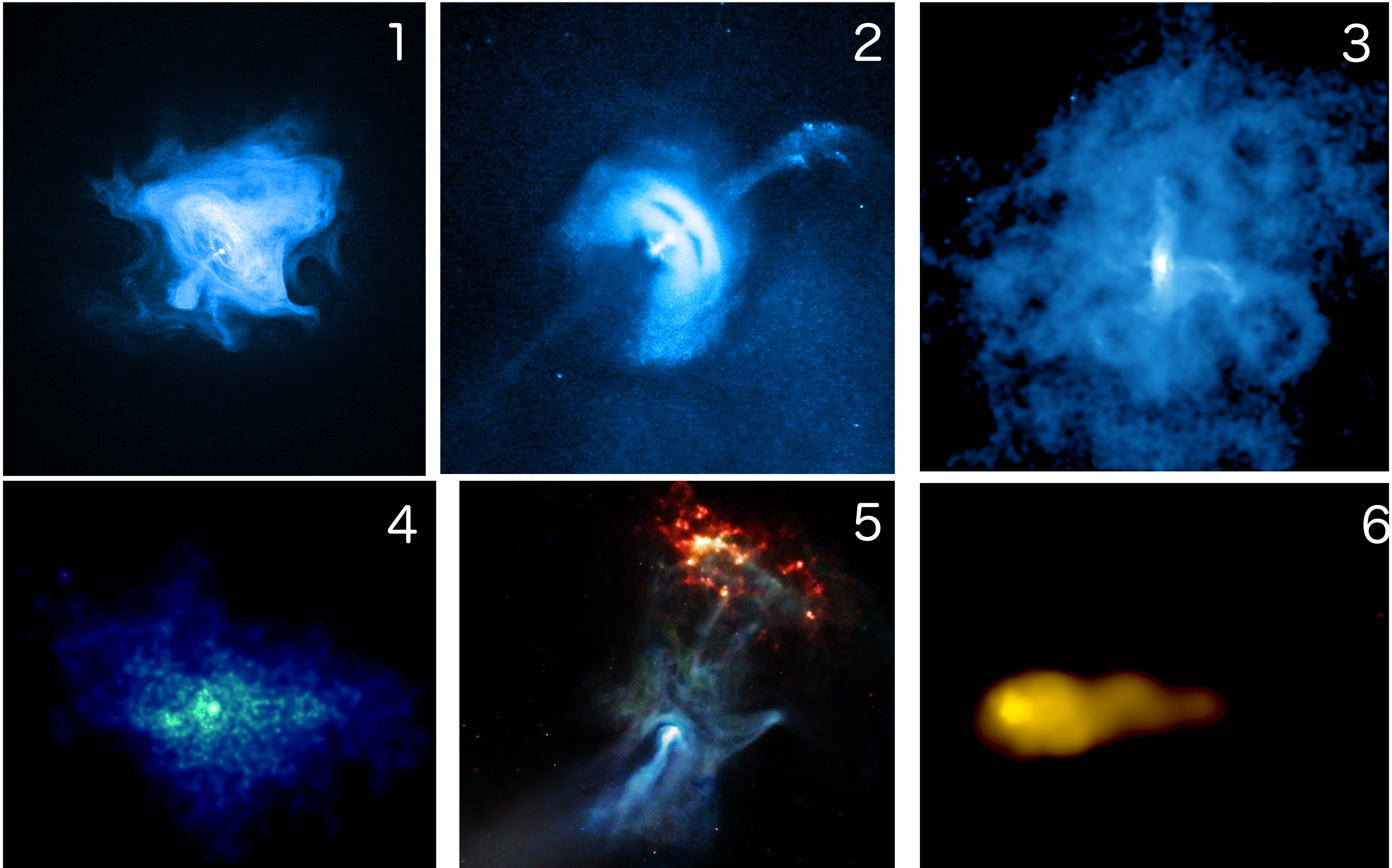

1: PSR B0531+21(Crab)、2: PSR B0833-45(Vela)、3: PSRJ0205+6449、
4: PSR J1930+1852、5: PSR B1509-58、6: PSR J1747--22958

PWNe are TeV γ-ray persistent sources

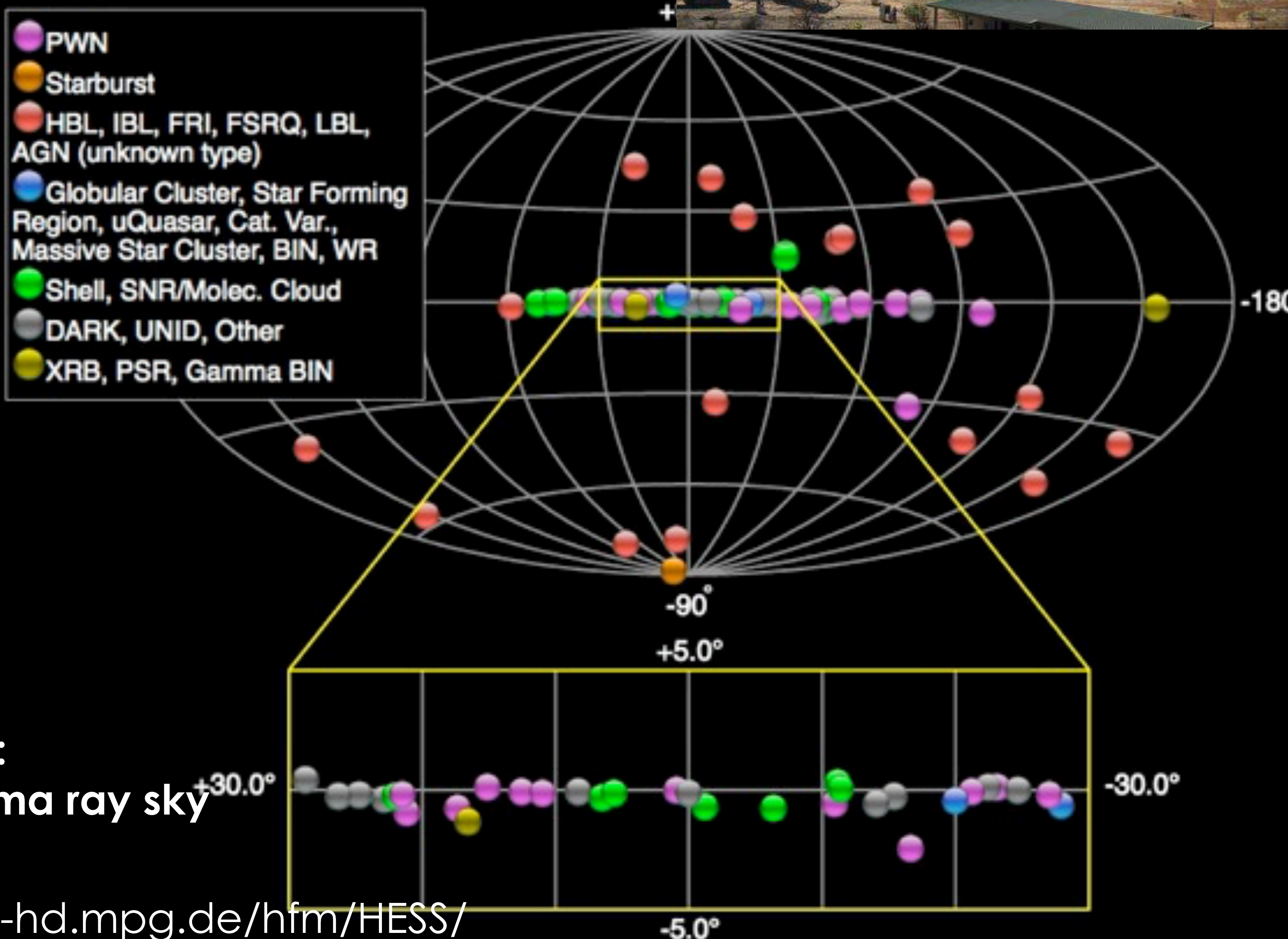

10th Anniversary:
The H.E.S.S. gamma ray sky
September 2012

https://www.mpi-hd.mpg.de/hfm/HESS/

Pulsar: Rotation power (spin-down power)

Magnetic rotating neutron star, which is 10km in size, is an electric power generator. As a back reaction of emission, the NS spins down.

https://fermi.gsfc.nasa.gov

Observable

$$L_{\rm rot} = \Im \Omega \dot{\Omega} \approx \frac{\mu^2 \Omega^4}{c^3}$$

$$\mu = \sqrt{c^3 \Im \dot{\Omega} / \Omega^3}$$

$\sim 10^{12}$ G

Correlation between X-ray Luminosity L_x and the spin-down Luminosity $L_{rot} = I\,\Omega\,(d\Omega/dt) \sim \mu^2\Omega^4/c^3$

$L_\gamma \propto L_{rot}^{1/2}$

$L_x \propto L_{rot}$

secondary particles?

$\log L_\gamma$

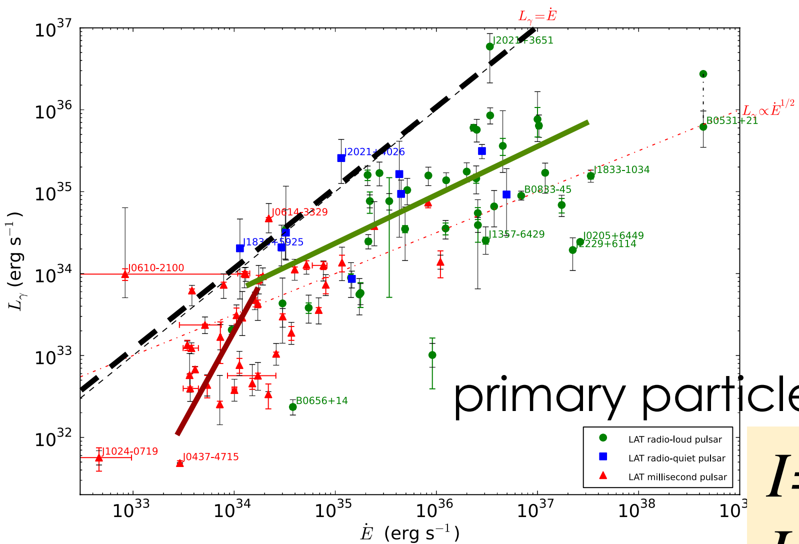

primary particles

$I = \mu\Omega^2/c$

$L_\gamma = IV_1$

$\log L_{rot}$

$\log L_x$

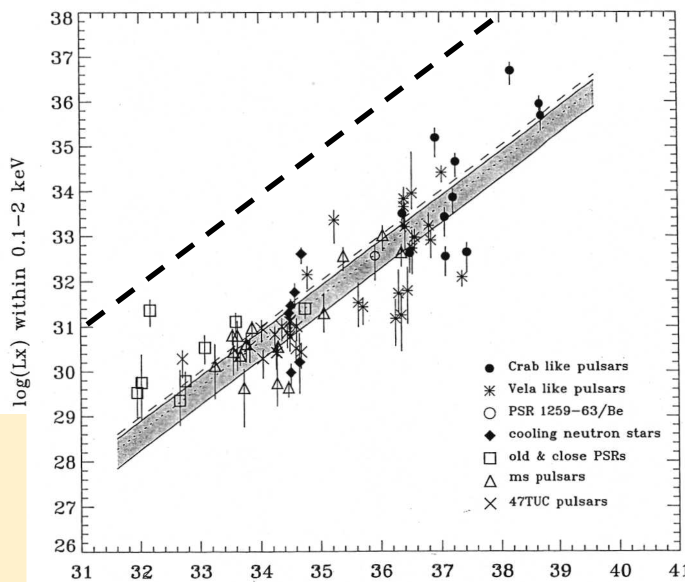

$\log L_{rot}$

The Second Fermi Large Area Telescope Catalog of Gamma-ray Pulsars (The Fermi-LAT collaboration 2013) apjs, 208,2

Becker, W. 2009, Astrophysics and Space Science Library, 357, 91

$L_{rad} - L_{rot}$ correlation: no

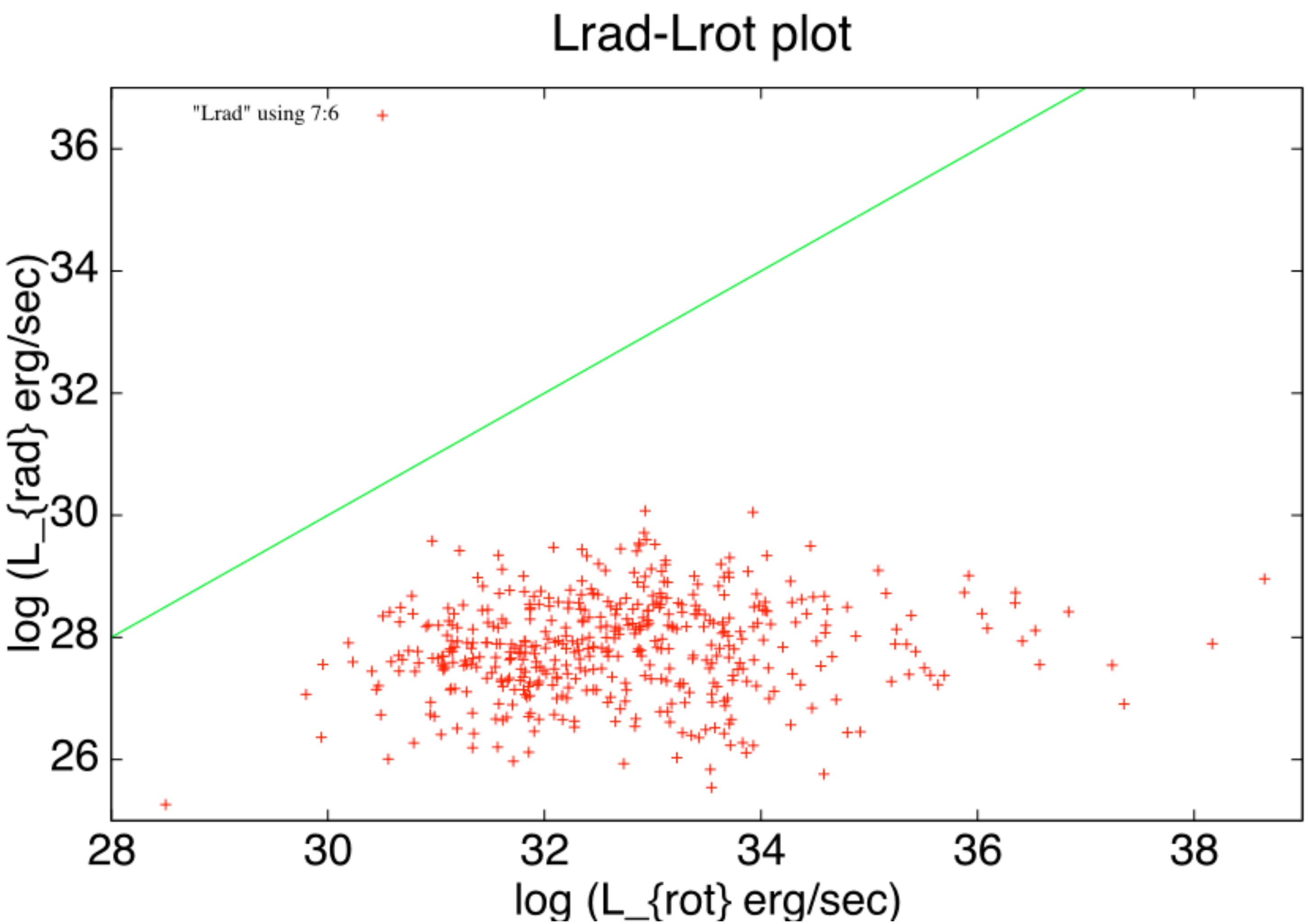

data from ATNF pulsar catalogue 400MHz+1400MHz

Unipolar Inductor

1821 M. Faraday

Unipolar inductor:

rotating magnet produces emf

Note $\partial B / \partial t = 0$

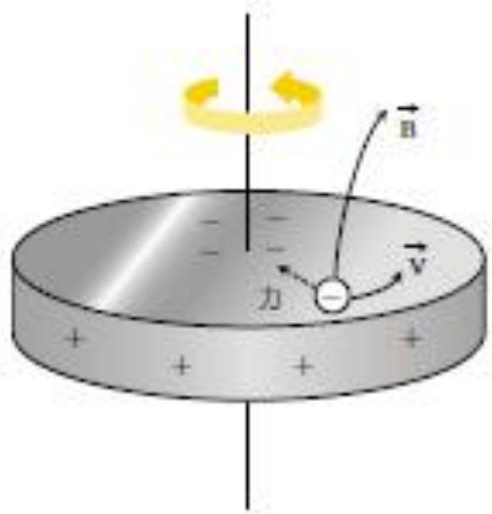

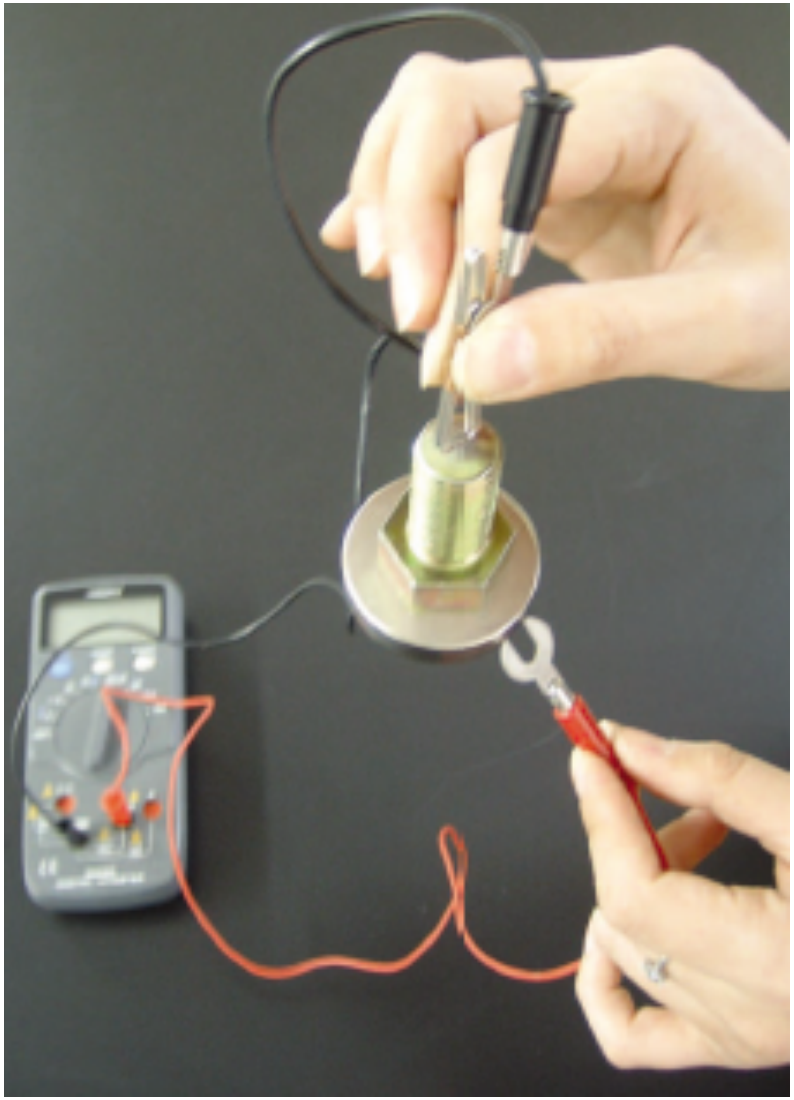


HIOKI
00.00 μA
RANGE
H.AUTO
50μA
Ω
μA

Model of the RPP

Simple understanding and standard model

By making a closed current circuit, one can extract energy, lighting the lamp.

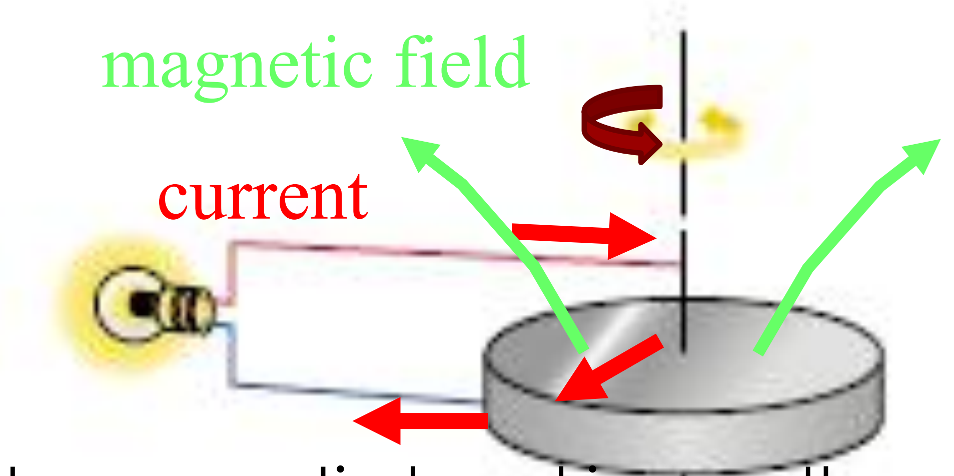

As a back reaction, electromagnetic breaking on the magnet causes spin-down: Thus rotational energy of the neutron star

$$E_{rot} = \frac{1}{2}\Im\Omega^2 = 2.0 \times 10^{50}\Im_{45}\left(\frac{P}{10\mathrm{msec}}\right)^{-2} \mathrm{erg}$$

is extracted.

Particle acceleration mechanism

$$\begin{cases} E_{||} \text{ driven} \\ E_{\perp} \text{ driven} \end{cases}$$

Equation of motion: for a plasma in the pulsar magnetosphere, the force balance on unit volume may be represented by

$$(\text{inertia}) = \rho_e \boldsymbol{E} + \frac{\boldsymbol{j} \times \boldsymbol{B}}{c} + (\text{non-electromagnetic forces})$$

Because the electromagnetic force dominates,

$$\boldsymbol{E} = \boldsymbol{E}_\perp, \ \boldsymbol{E}_\parallel = 0$$ (magnetic field lines are iso-potentials)

($E\perp$ x B causes rotation with the star)

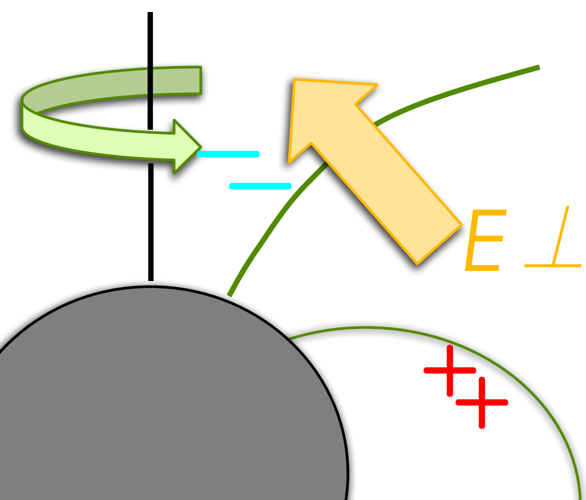

This is almost perfect for most of astrophysical plasmas, except for pulsars because …

$$\rho_e = \frac{\nabla \cdot \boldsymbol{E}_\perp}{4\pi}$$ ~10^{12} particles/cm^3

Look at Poisson equation and
pay attention to how plasma is supplied
to the magnetosphere

Prescription

$$\boldsymbol{E}_c = -(\Omega \times \boldsymbol{r}) \times \boldsymbol{B}/c$$

define corotation electric field

$$\rho_{gj} = \nabla \cdot \boldsymbol{E}_c/4\pi$$ Goldreich-Julian charge density

$$\boldsymbol{E}' = \boldsymbol{E} - \boldsymbol{E}_c$$ the difference

$$\boxed{\nabla \cdot \boldsymbol{E}' = 4\pi(\rho_e - \rho_{gj})}$$

‘’ If the space charge density differs from the GJ density, then E// apperas.’’

If $\boldsymbol{E}_{\parallel} = 0$
(plasma is sufficiently supplied),

$$\boldsymbol{v}_D = c\frac{\boldsymbol{E}_c \times \boldsymbol{B}}{B^2} = \Omega \times \boldsymbol{r} = \Omega r \sin\theta$$

$v \to c$

$$\boxed{R_L = c/\Omega}$$

light cylinder is a singularity

γm grows so large as centrifugal force drives an out flow

E$\perp$ drives this singularity

current understanding
of the pulsar magnetosphere

Electrosphere

start
with surrounding

vacuum

For the first time, the particle simulation is applied for this situation by Krause-Polstorf and Michel (1985).

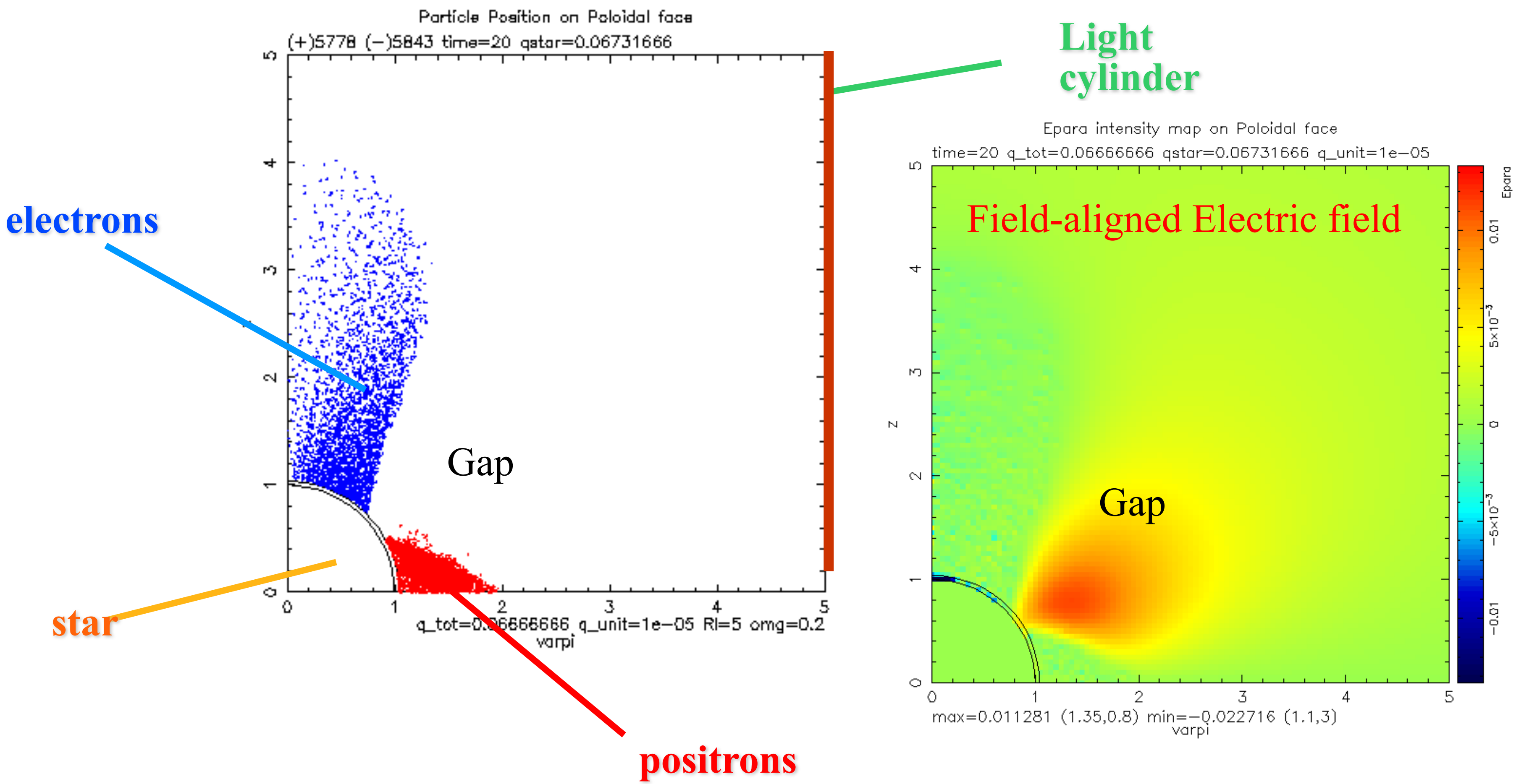

These pictures are reproduced by our code.

pair creation

gamma-ray + B ➔ $e^+ + e^-$

gamma-ray + X-ray ➔ $e^+ + e^-$

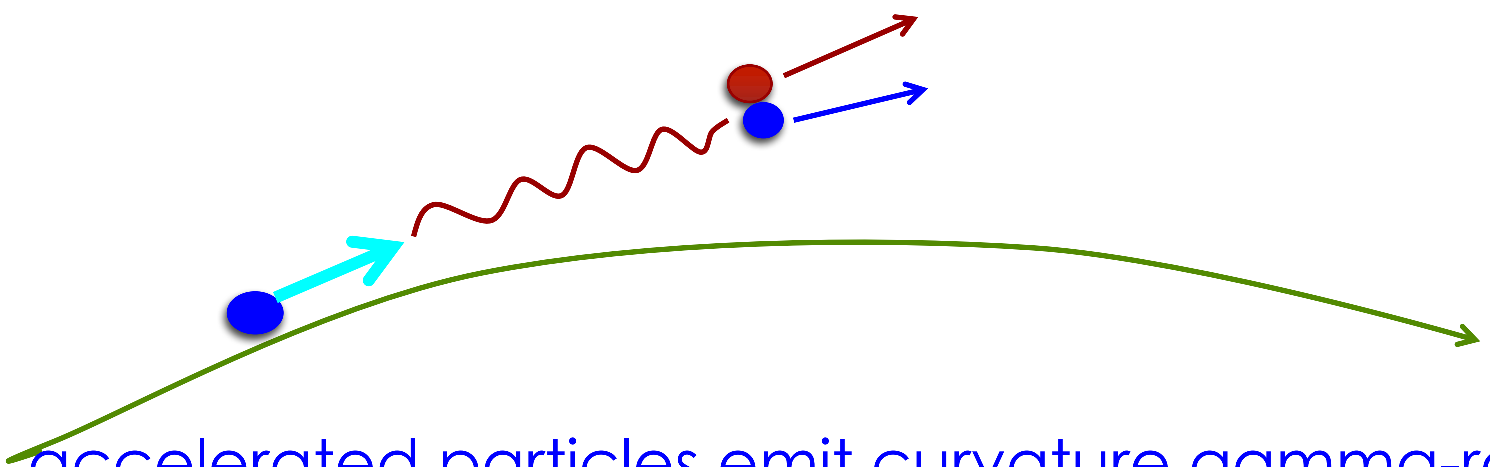

accelerated particles emit curvature gamma-rays

Outer Gap

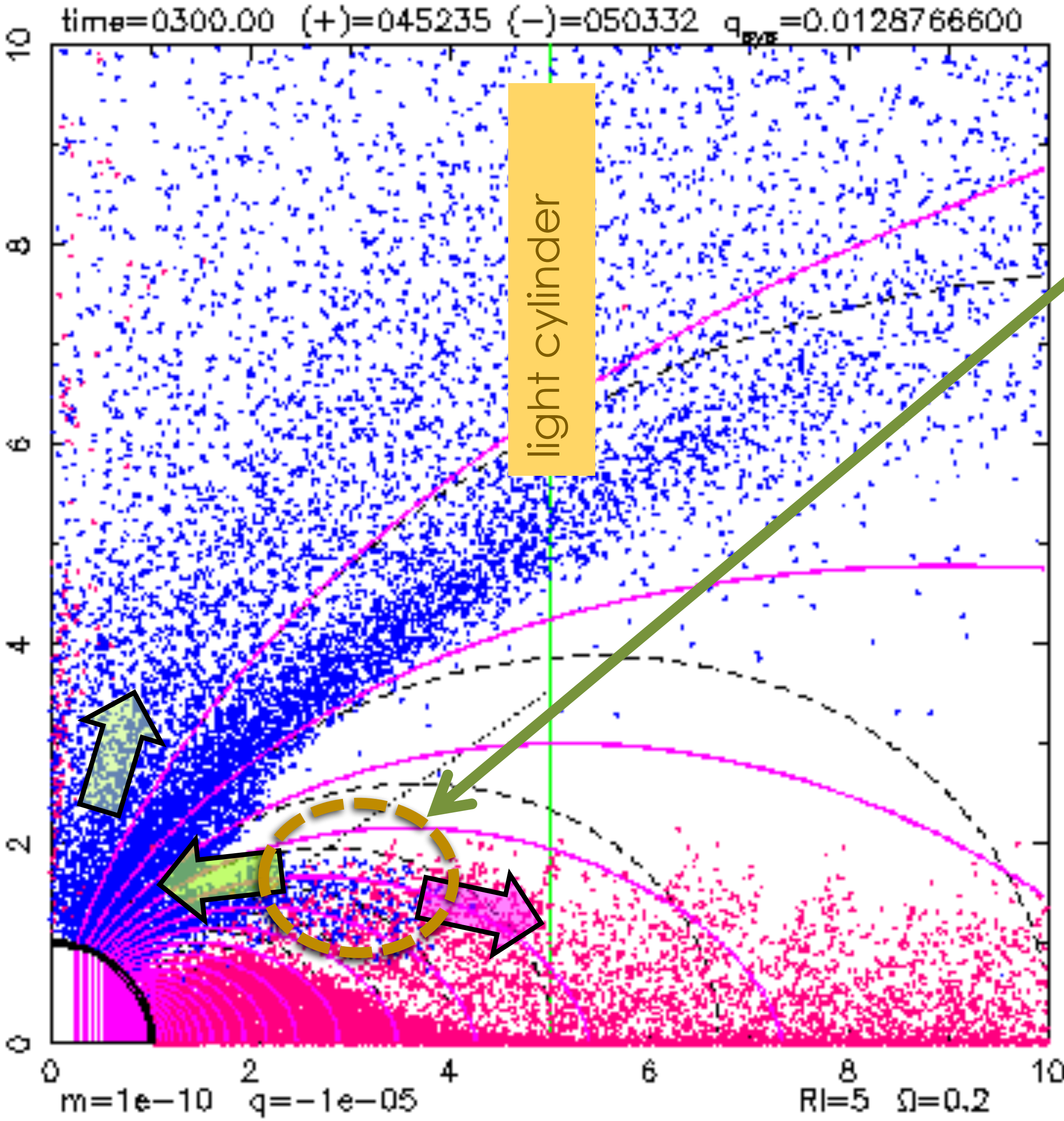

outer gap

Pairs are continuously produced.

Pairs are immediately separated by the field-aligned electric field.

E// map

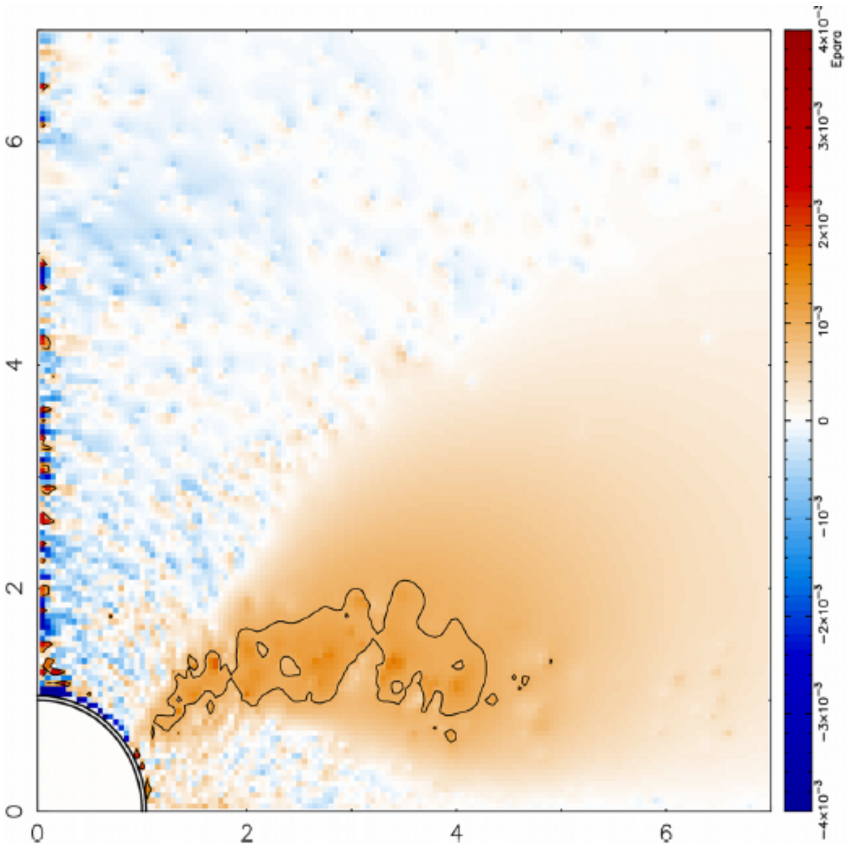

Because we have plasma sources, E// is screened out everywhere, except for the outer gap where E// is just above Ec: necessary minimum for pair creation.

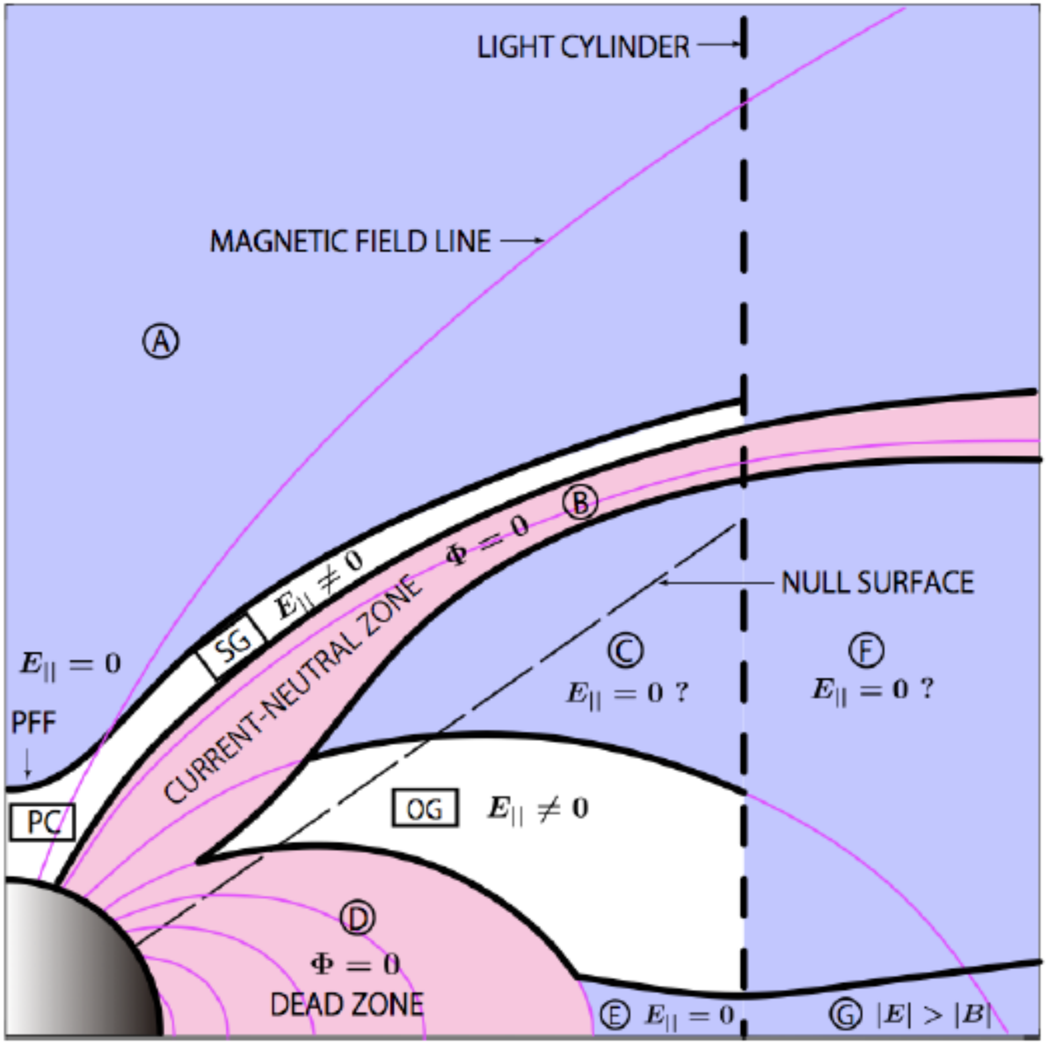

after Yuki, S., Shibata, S., 2012, PASJ, 64, 43

Dead zones along "current-neutral zone" is found. PC,SG locate above it and OG below it.

The outer gap is sandwiched by two dead zones. Therefore, the boundary conditions used previously in the outer gap is correct.

force-free model

$$\rho\mathbf{E} + \frac{\mathbf{J} \times \mathbf{B}}{c} = \mathbf{0},$$

The Axisymmetric force-free Magnetosphere CKF model 1999

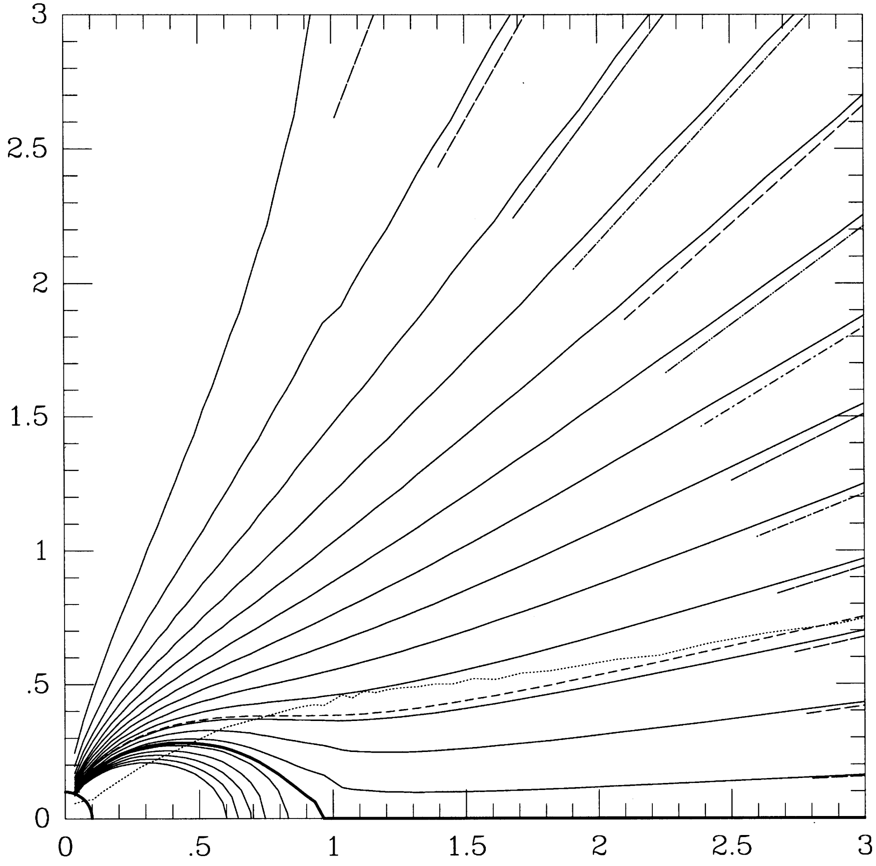

Contopoulos, I., Kazanas, D., & Fendt, C. 1999, ¥apj, 511, 351

$$\left(1-\frac{R^2}{R_{\rm LC}^2}\right)\left(\frac{\partial^2\Psi}{\partial R^2}+\frac{\partial^2\Psi}{\partial z^2}\right)-\left(1+\frac{R^2}{R_{\rm LC}^2}\right)\frac{1}{R}\frac{\partial\Psi}{\partial R}+I\left(\Psi\right)\frac{\partial I}{\partial\Psi}=0.$$

force-free model (1)

healthy approximation!!!(?)

1. structure: open/close region
   + current sheets
2. why open field? ←current sheet ←BC
3. BC: dipole at the center
   open field at infinity
   outward current +inward current =0 (closed current system)
   regular on the light cylinder so that the current function is chosen ←ill method?

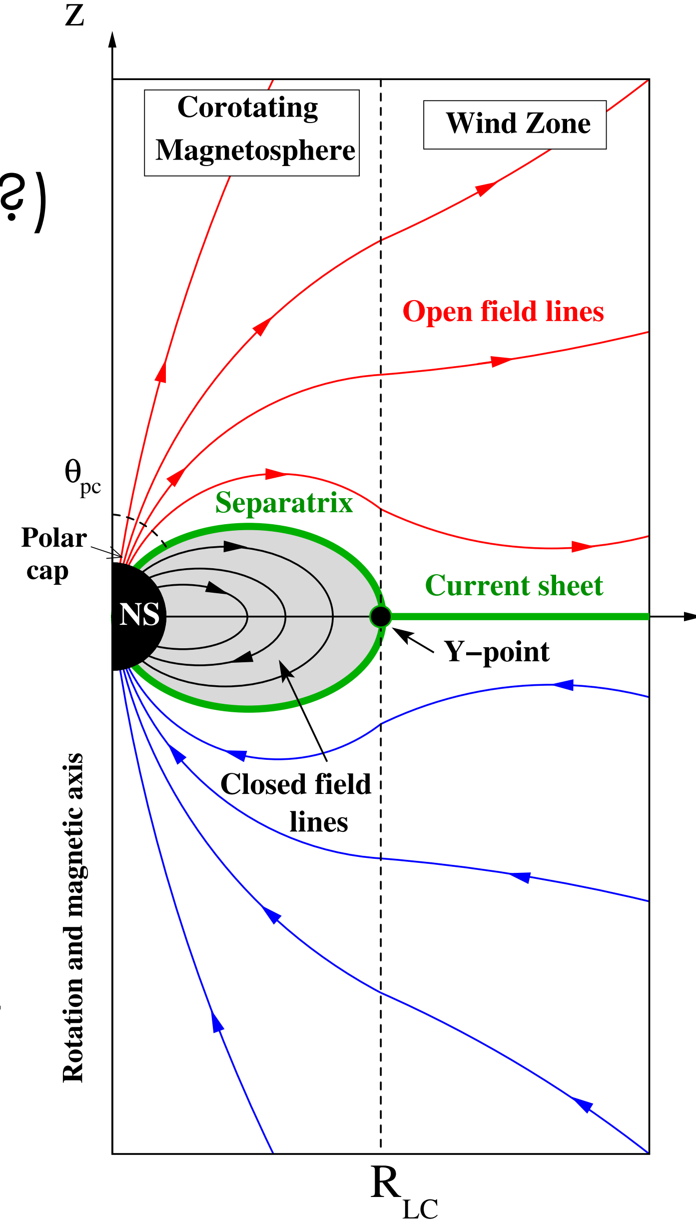

force-free model (2)

healthy approximation!!!(?)

4. separatrix, surface charge ← might disappear in dissipative current sheet

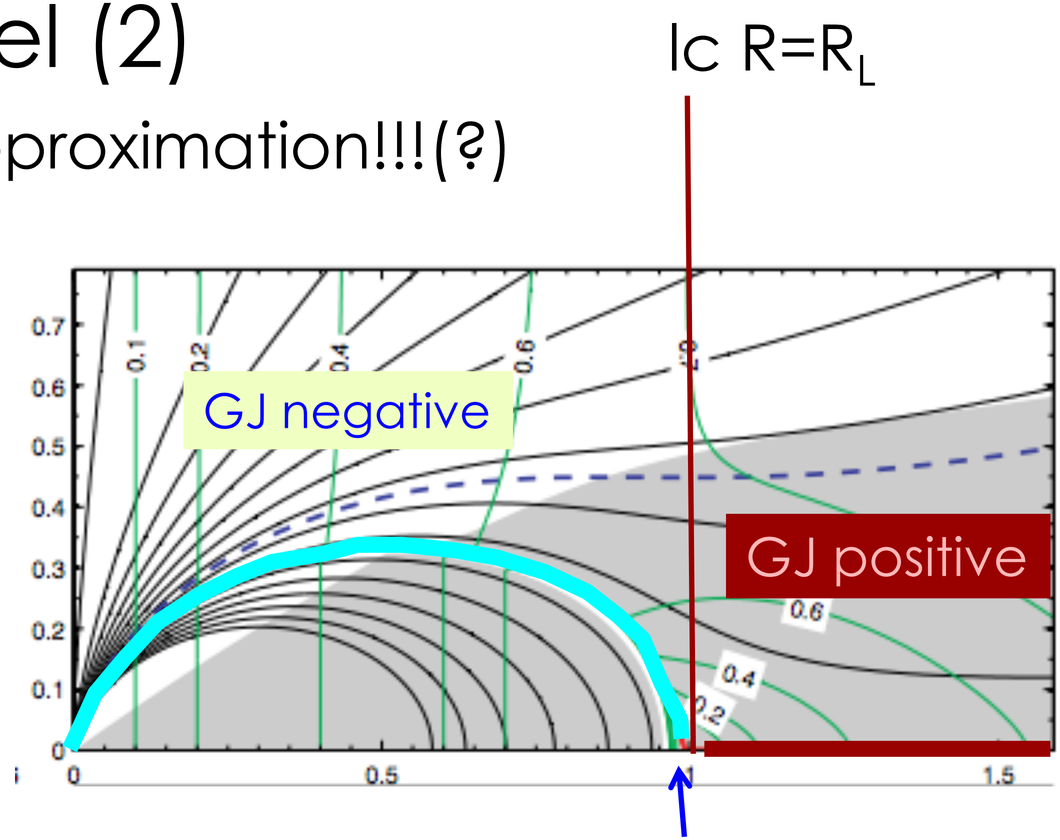

5. force-free solution is one parameter family w.r.t. X_Y. As $X_Y \rightarrow R_L$, volume of the return current increases, but never $X_Y=1$ due to plasma inertia.

covering a curved surface with flat paper

covering a curved surface with flat paper

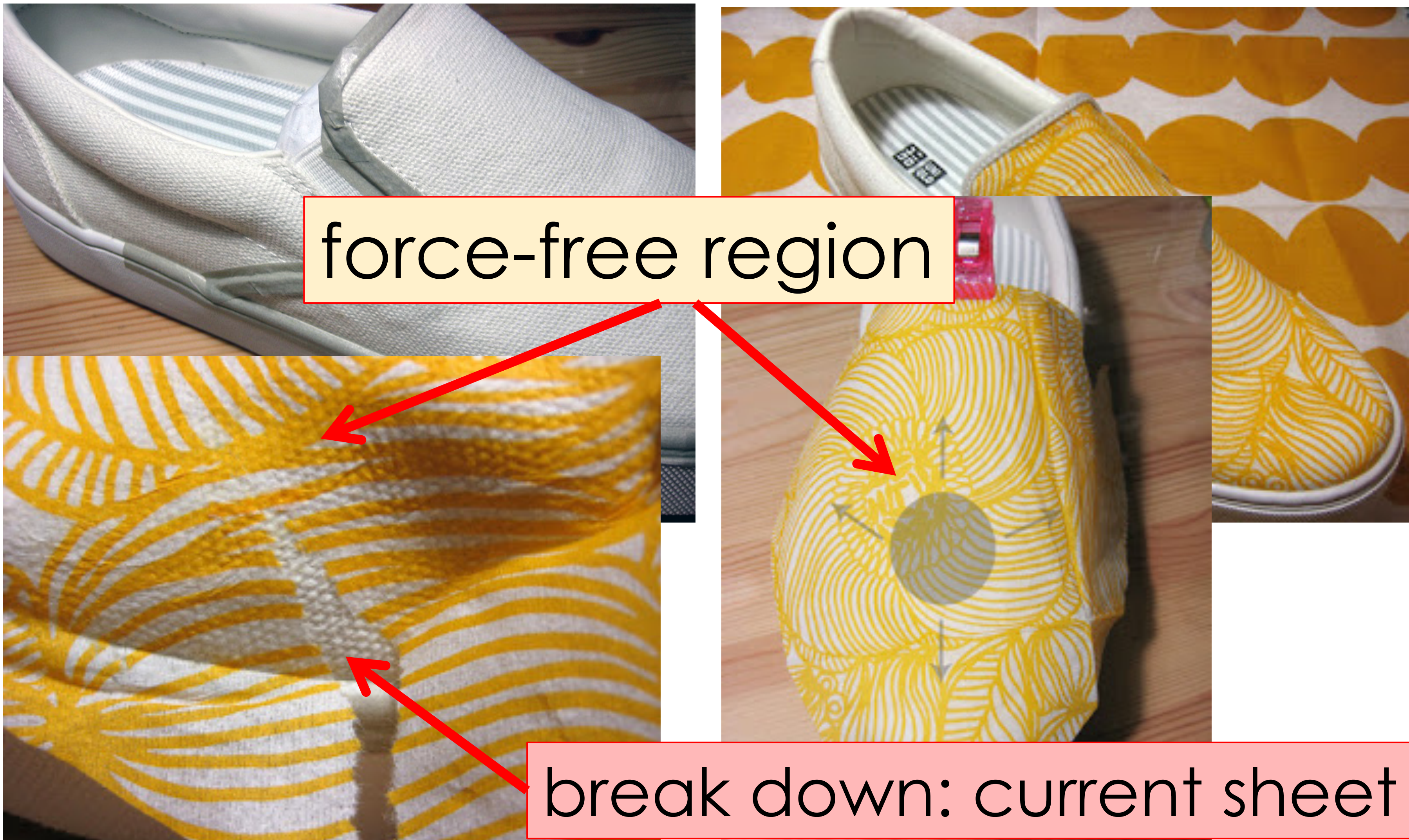

force-free

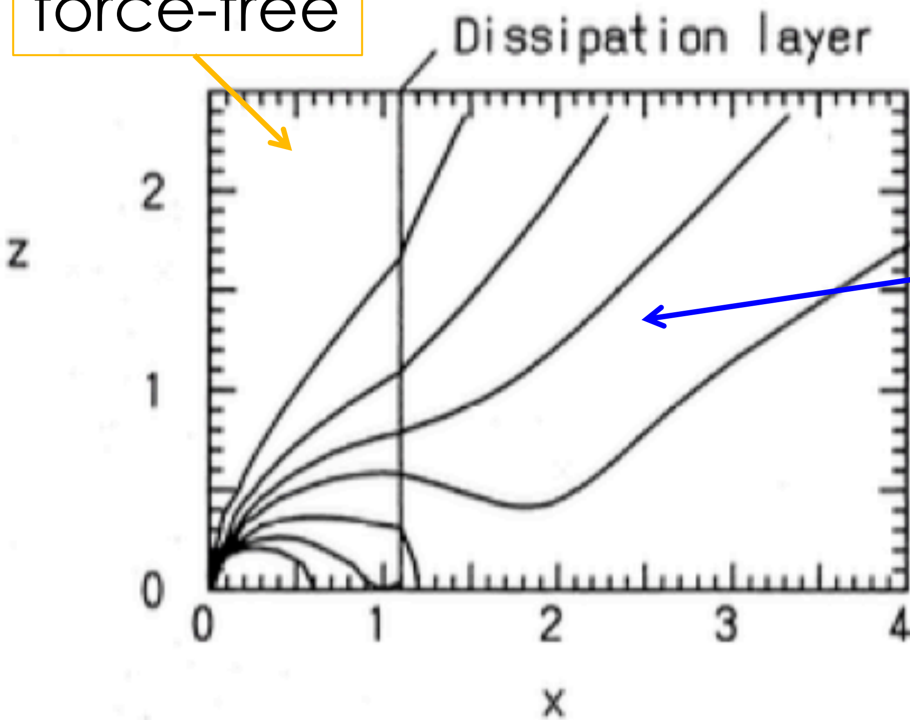

MHD
(with intertia of material
without dissipation)

Figure 5. The magnetic field structure for the global model with $\beta = 0.877$ and $\hat{S}_{out} = 0.9$. The thin dissipation layer is located at $\hat{x} = 1.1$, where the jump conditions are imposed. Within the layer the field is approximated to be force-free, while beyond the layer the dissipation-free wind with finite inertia is adopted. The poloidal current emerges at low latitudes and returns at high latitudes. Some of the current flows to infinity before returning to the star, but some returns via the dissipation layer. The layer loses energy and angular momentum via radiation. The layer has finite thickness with a B-field-aligned electric field component, so that the angular velocity of the wind is less than that of the inner, force-free domain.

Mestel, L., & Shibata, S. 1994, mnras, 271, 621

force-free model (3)

healthy approximation!!!(?)

Voltage in open magnetic flux is utilizable:

$$V_0 \sim B_L R_L = \mu\Omega^2/c^2$$

$$\gamma_0 = eV_0/mc^2$$

Open flux determines polar cap size:

$$R_{pc} \approx \left(\frac{R_*}{R_L}\right)^{1/2} R_*$$

force balance determines the current:

$$I_0 \sim R_L^2 \boldsymbol{j}_p = \mu\Omega^2/c$$

Rotation power is thus determined as

$$L \approx \frac{\mu^2\Omega^4}{c^3}$$

time-dependent force-free simulation for oblique rotators

time-dependent force-free simulation for oblique rotators

$$\rho_e \boldsymbol{E} + \frac{1}{c}\boldsymbol{j} \times \boldsymbol{B} = 0 \qquad \longleftarrow \qquad \rho_e = \nabla \cdot \boldsymbol{E}/4\pi$$

$$\boldsymbol{j} = c\rho_e \left(\frac{\boldsymbol{E} \times \boldsymbol{B}}{B^2} \right) + \frac{c}{4\pi} \frac{\boldsymbol{B} \cdot \nabla \times \boldsymbol{B} - \boldsymbol{E} \cdot \nabla \times \boldsymbol{E}}{B^2} \boldsymbol{B}$$

$$\boxed{\begin{aligned} \frac{1}{c}\frac{\partial \boldsymbol{E}}{\partial t} &= \nabla \times \boldsymbol{B} - \frac{4\pi}{c}\boldsymbol{j} \\ \frac{1}{c}\frac{\partial \boldsymbol{B}}{\partial t} &= -\nabla \times \boldsymbol{E} \end{aligned}}$$

current sheets are formed, but numerically dissipates.

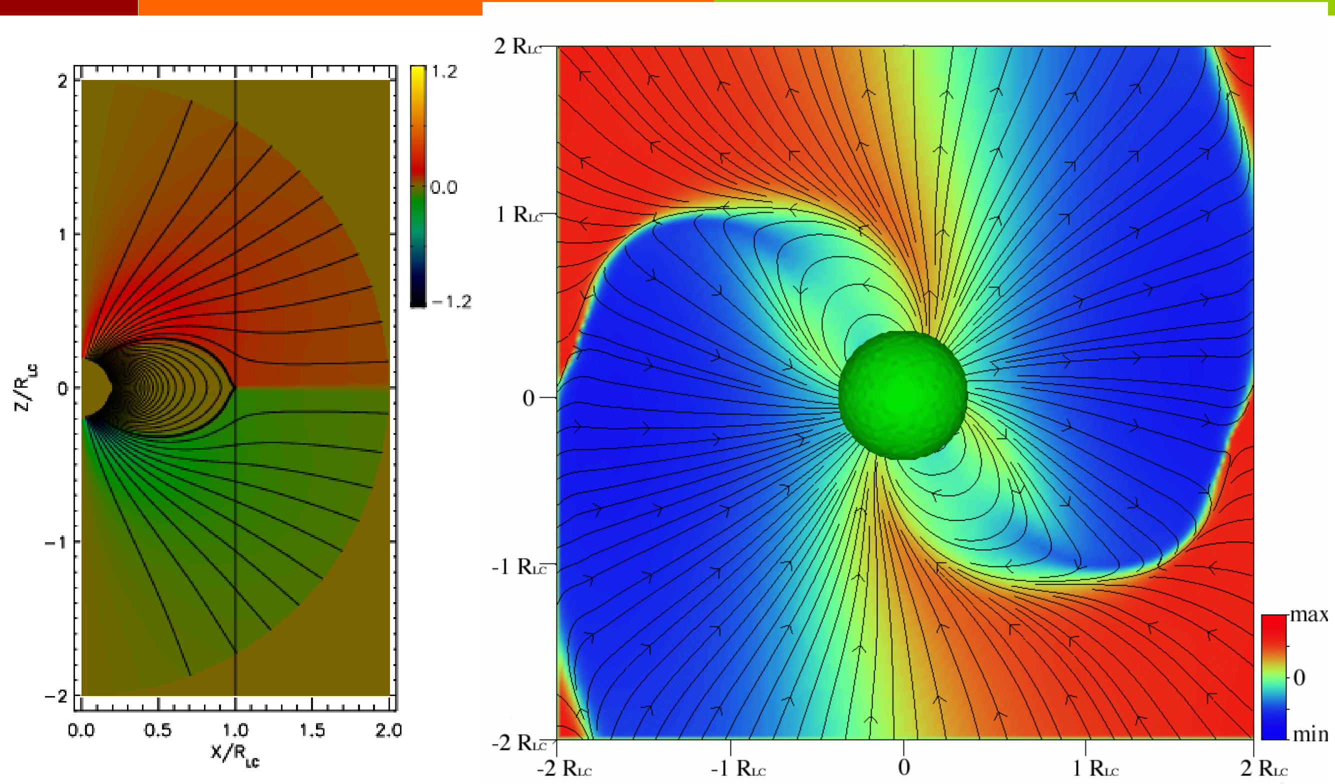

Fig. 5 Snapshots of time-dependent force-free simulations of the aligned (left) and oblique (right) rotators (from Spitkovsky 2006). The oblique rotator magnetosphere is shown in the $\mathbf{\Omega} - \boldsymbol{\mu}$ plane; the inclination angle is $\chi = 60^o$. Solid lines represent magnetic field lines, and color shows the strength of the magnetic field component perpendicular to the plane of the figure (the toroidal field in the aligned rotator case).

$$L \approx \frac{\mu^2 \Omega^4}{c^3}(1 + \sin^2 \alpha)$$

Non force-free magnetosphere

toward the realistic model

$\boldsymbol{E}_{\|}$ Acceleration

1. Assuming no pair production, one may obtain E// acceleration with $\nabla \cdot \boldsymbol{E}' = 4\pi(\rho_e - \rho_{gj})$

2. once E// accelerate particles, pair creation follows and in the next step, E//will be screened out.

3. Because pair-creation stops and flows out, the situation turns back to the initial state.

particle acceleration and pair-creation will be intermittent.
maybe mild acceleration persistently?

$$\nabla \cdot \boldsymbol{E}' = 4\pi(\rho_e - \rho_{gj})$$

The difference of the space charge density from the GJ density produces E//.

The space charge density is linked to the current density which is determined by the global dynamics. Thus the problem is somewhat complicated,….

Possible E// acceleration, pair creation sites

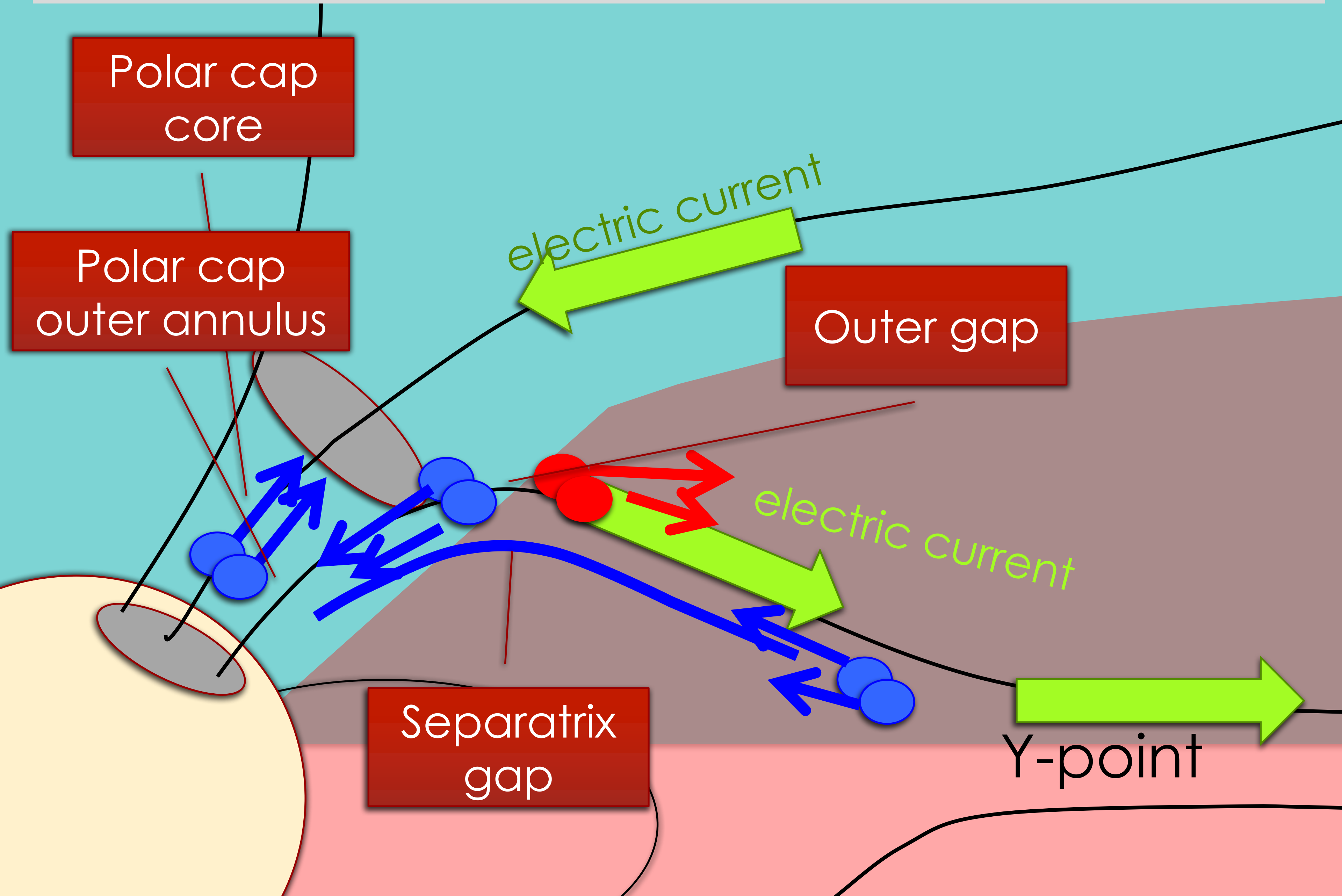

Numerical global particle simulation

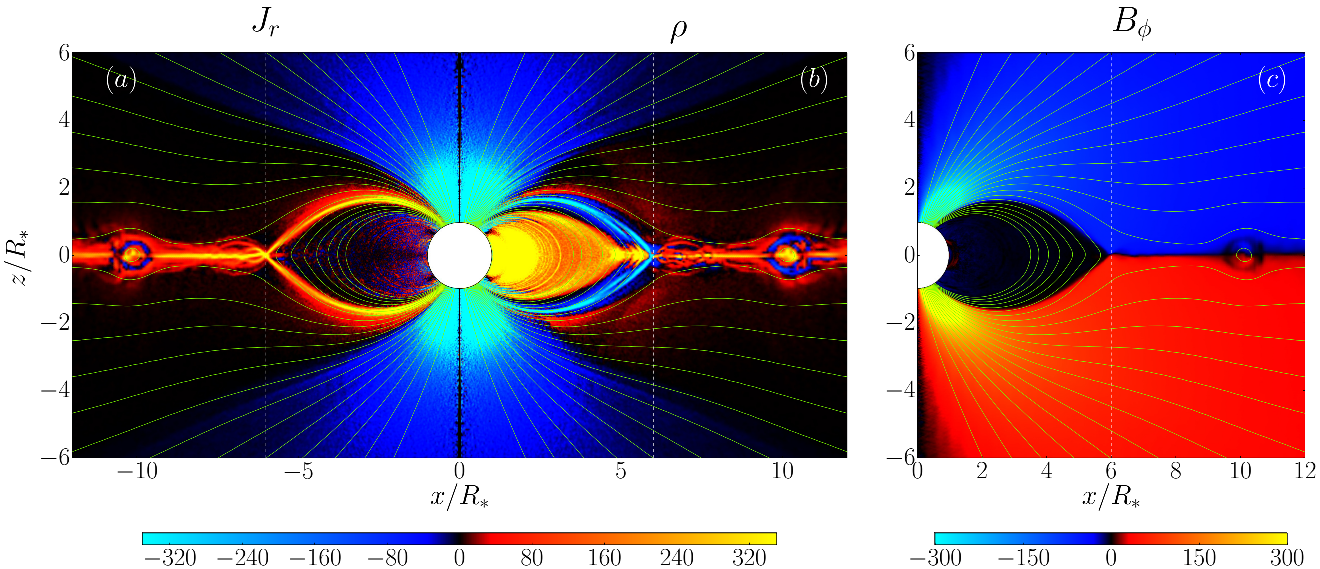
J_r
ρ
B_ϕ
(a)
(b)
(c)
z/R_*
x/R_*
x/R_*
−320 −240 −160 −80 0 80 160 240 320
−300 −150 0 150 300

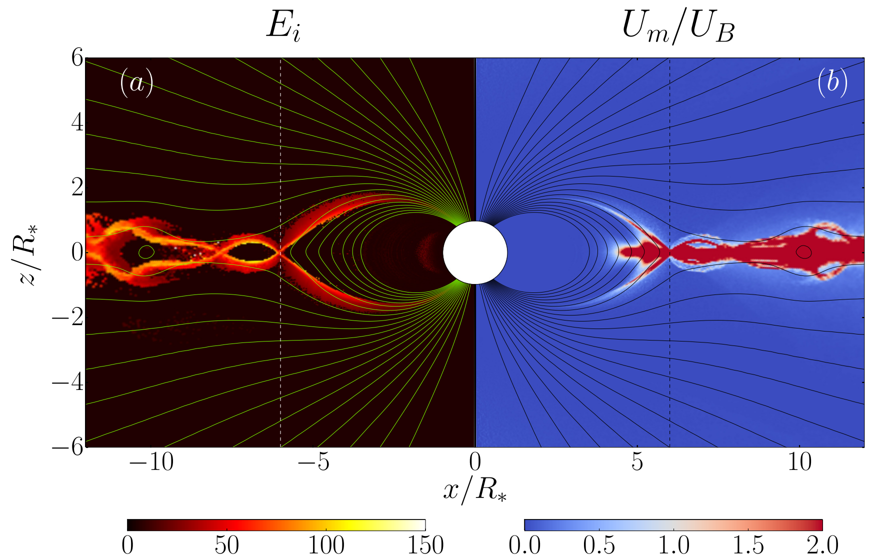
E_i
U_m/U_B
(a)
(b)
z/R_*
x/R_*
0 50 100 150
0.0 0.5 1.0 1.5 2.0

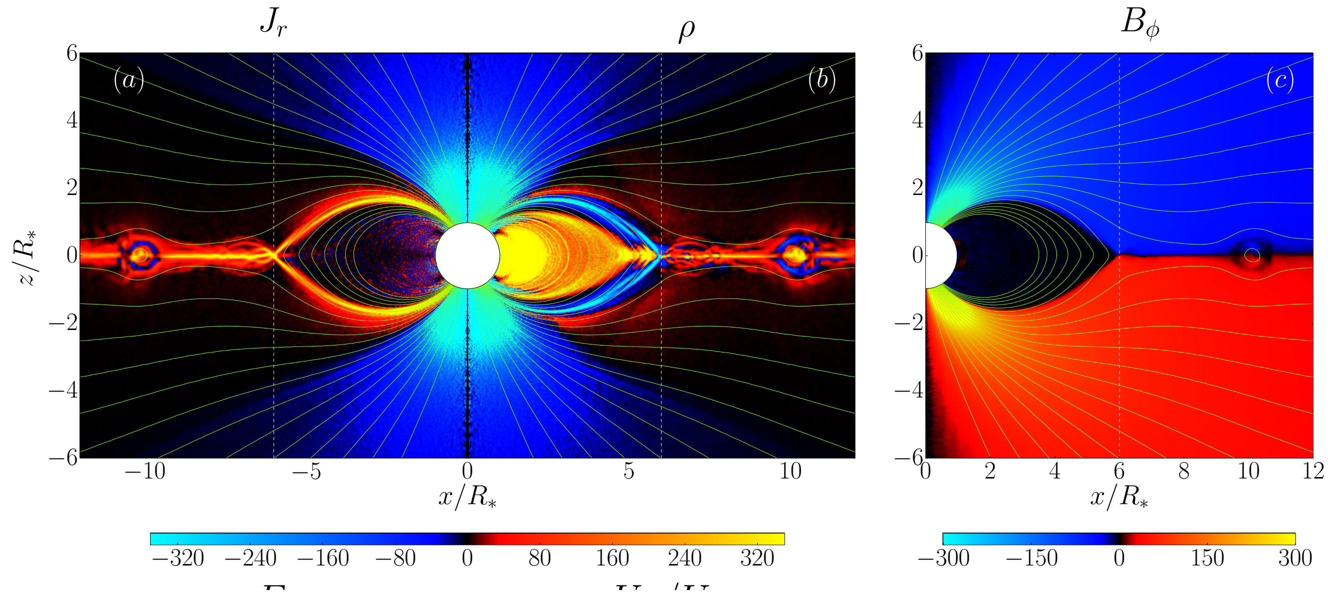

1. part … creation take plac … aratrix
2. +pa … emispheres and … hanging thet
3. -par
4. spin- … with the resu … d to plasma kinetic energy for the aligned rotator. This rate

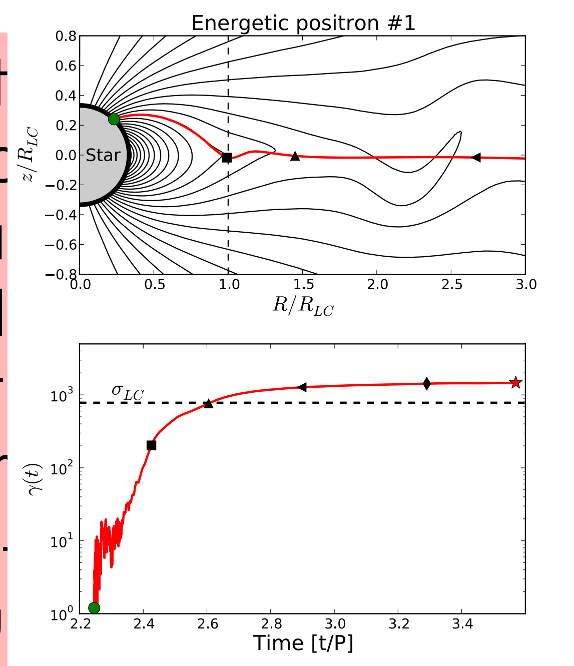

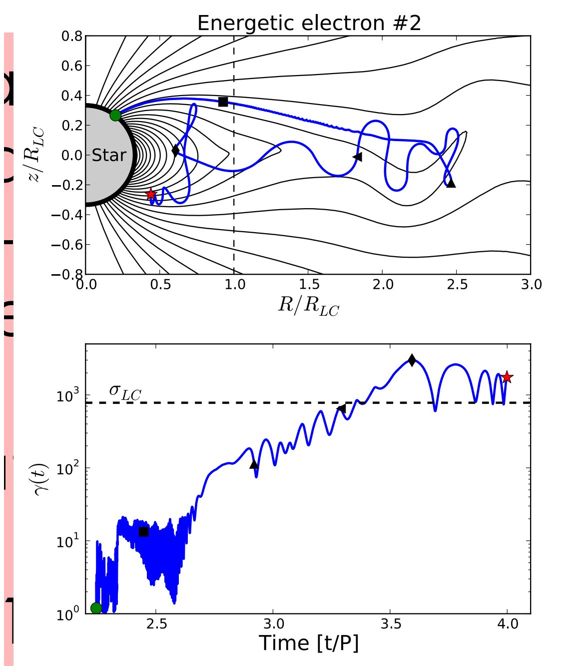

Current Sheet with Dissipation

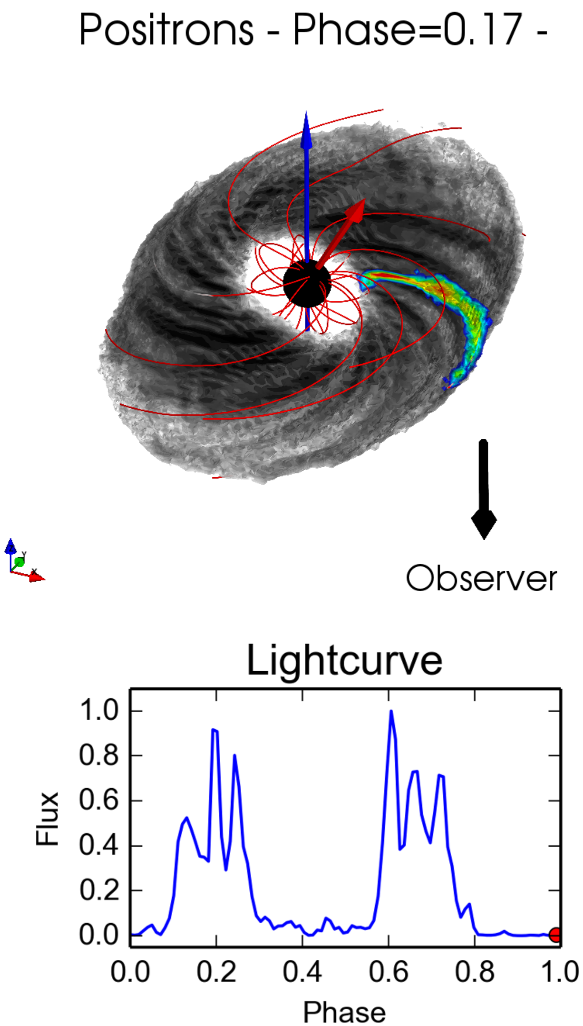

Fig. 11 **Top:** Spatial distribution of the high-energy synchrotron radiation from an oblique rotator obtained with a 3D PIC simulation. The grey scale shows the isotropically integrated flux, while the color scale shows the emitting regions at the pulsar phase 0.17 as seen by an observer looking along the equator. The angle between the rotation axis (blue arrow) and the magnetic axis (red arrow) is $\chi = 30^o$. Red curves are the magnetic field lines. **Bottom:** Reconstructed high-energy pulse profile of radiation received by the observer. Figure adapted from Cerutti et al. (2016b).

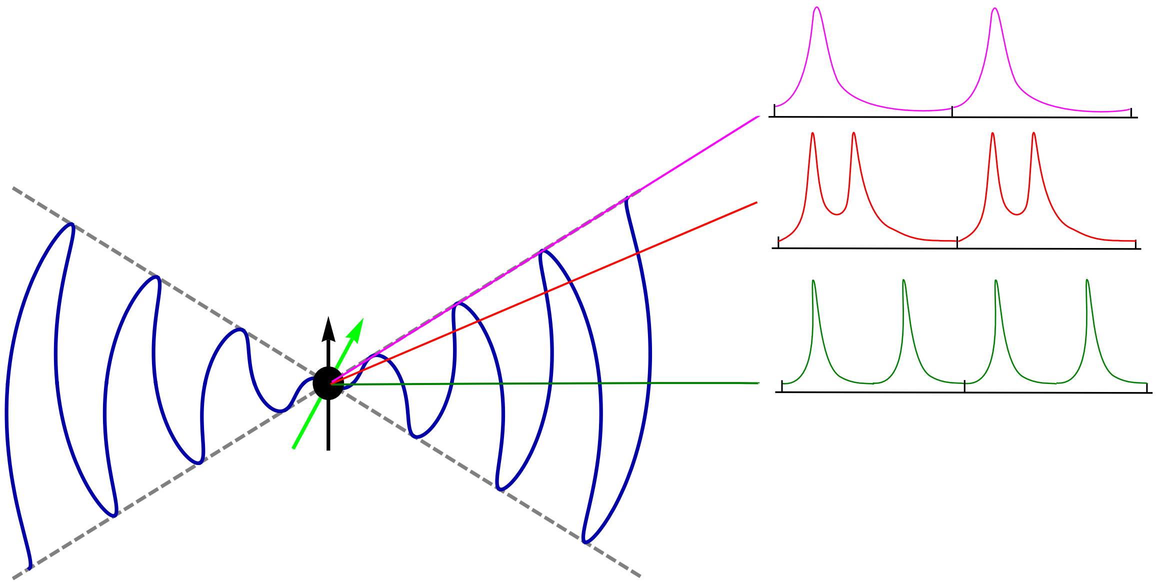

Fig. 1.2 Lightcurves from the wind. A distant observer can detect a pulse of emission when the expanding current sheet passes the radius r_0 along his line of sight. The emissivity of this sheet quickly diminishes afterwards. Depending on the viewing angle, the observer can detect up to two pulses per rotational period of a pulsar.

Pulsar striped winds
¥bibitem[Mochol(2017)]{2017arXiv170200720M} Mochol, I.¥ 2017, arXiv:1702.00720

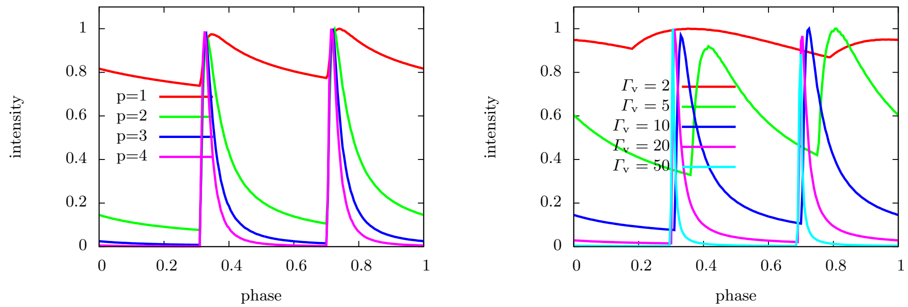

FIGURE 16. Sample of synchrotron emission light curves for different power law indices $p = \{1, 2, 3, 4\}$ with $\Gamma_\mathrm{v} = 10$ on the left and for different Lorentz factors $\Gamma_\mathrm{v} = \{2, 5, 10, 20, 50\}$ with $p = 2$ on the right. Intensities are normalized to $I_\mathrm{max} = 1$.

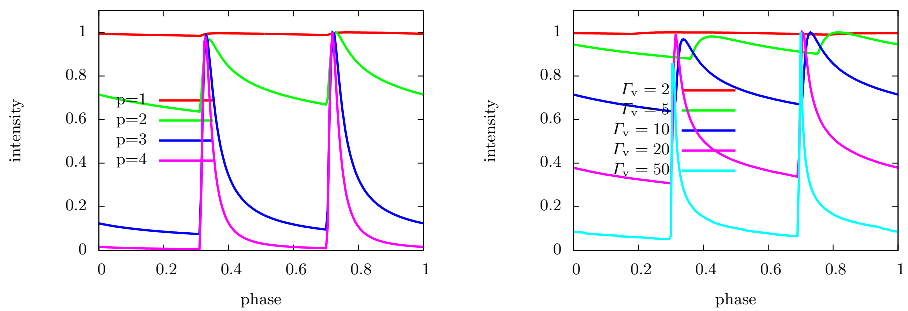

FIGURE 17. Sample of inverse Compton emission light curves for different power law indices $p = \{1, 2, 3, 4\}$ with $\Gamma_\mathrm{v} = 10$ on the left and for different Lorentz factors $\Gamma_\mathrm{v} = \{2, 5, 10, 20, 50\}$ with $p = 2$ on the right. Intensities are normalized to $I_\mathrm{max} = 1$.

$$I_\nu(t) = \int_{-\infty}^{+\infty} \int_{R_0}^{+\infty} \int_{\pi/2-\chi}^{\pi/2+\chi} \int_0^{2\pi} j_\nu(\mathbf{r}, t')\, \delta(r - r_s(\vartheta, \varphi, t')) \times$$

$$\times\, \delta\left(t' - (t - \frac{||\mathbf{R}_\mathrm{obs} - \mathbf{r}||}{c})\right) r^2 \sin\vartheta\, dt'\, dr\, d\vartheta\, d\varphi\ .$$

$$j_\nu^\mathrm{sync}(\mathbf{r}, t) = K_e(\mathbf{r}, t)\, \nu^{-(p-1)/2}\, \mathcal{D}^{(p+3)/2}\, B^{(p+1)/2} \qquad (8.24a)$$

$$j_\nu^\mathrm{IC}(\mathbf{r}, t) = K_e(\mathbf{r}, t)\, \nu^{-(p-1)/2}\, \mathcal{D}^{p+2}\, n_\gamma(\varepsilon) \qquad (8.24b)$$

Relativistic beaming effects are symbolised by the usual Doppler factor

$$\mathcal{D} = \frac{1}{\Gamma_\mathrm{v}\,(1 - \boldsymbol{\beta}_\mathbf{v} \cdot \mathbf{n}_\mathrm{obs})}\ . \qquad (8.25)$$

Summary in Jan. 2018

1. Rotation power is approximately given by
$$L \approx \frac{\mu^2 \Omega^4}{c^3} \left(1 + \sin^2 \chi\right).$$
2. particle acceleration by E// (non-ideal-MHD) is essential.
3. Simulations by non-MHD and PIC are strong tool, but
4. Acceleration site is still unidentified
   - Y-point - equatorial current sheet - outer gap
   - separatrix gap - polar caps
5. Radio emission mechanism: open question
6. Pulsar Wind: open question
7. Link between radio/timing and high-energy emission should be investigated.

thank you